傾斜機能圧電材料の感知・応答機構解明とマルチスケール性能評価

成田史生* 中川 淳**
進藤裕英** 水戸裕也**

Characteristics of Detection and Response in Functionally Graded Piezoelectric Materials and Multi-Scale Performance Evaluation

Fumio Narita*, Jun Nakagawa**, Yasuhide Shindo** and Yuya Mito**

We investigate both analytically and experimentally the sensitivity and activity of functionally graded piezoelectric materials under electromechanical loading. A phenomenological model of domain wall motion in alternating current electric fields is used, and a nonlinear finite element analysis is employed to discuss the effects of electromechanical loading, number of layers, and property gradation on the induced voltage, deflection and internal stresses for the piezoelectric cantilevers. Experimental results, which verify the model, are also presented using functionally graded piezoelectric bimorphs. Good agreement is obtained between the tests and predictions.

1. INTRODUCTION

Recent advances in piezoelectric materials processing and engineering have spurred the development of a new class of materials, called functionally graded piezoelectric materials (FGPMs), with promising applications in smart materials and structures. In these, the dissimilar piezoelectric materials with contrasting electromechanical properties are brought together to address the needs of aggressive environments of electromechanical loading. The piezoelectric properties are thus engineered to have a relatively smooth spatial variation, and the FGPMs pose new challenges in terms of modeling, characterization and optimization from the point of view of electromechanical characteristics[1]. One of the limitations for practical use of these piezoelectric materials and products is their nonlinear behavior, which occurs due to polarization switching[2] and/or domain wall motion[3] at high driving levels. In order to optimize the performance of the piezoelectric devices with functionally graded microstructure under these conditions, understanding of the nonlinear behavior in FGPMs is of great importance.

The objective of this work is to investigate the nonlinear characteristics, such as sensitivity and activity, of FGPMs under electromechanical loading. The functionally graded piezoelectric devices used consist of many thin soft piezoelectric layers. A simple phenomenological model of a vibrating domain wall in alternating current (AC) electric fields is used, and a nonlinear finite element analysis is performed to discuss the effects of electromechanical loading, number of layers, and property gradation on the induced voltage, deflection and internal stresses for the devices. Experimental results are also presented to validate the predictions using functionally graded bimorph-type bending sensors and actuators. Calculations show reasonable agreement with the experimental data.

2008年1月30日 受理
* 豊田理化学研究所研究嘱託
(東北大学大学院工学研究科)
** 東北大学大学院工学研究科

2. ANALYSIS

2.1. Basic equations

Consider the orthogonal coordinate system with axes x_1, x_2 and x_3. The basic equations for piezoelectric materials are

$$\sigma_{ji,j} = \rho u_{i,tt} \tag{1}$$

$$D_{i,j} = 0 \tag{2}$$

$$\varepsilon_{ij} = s_{ijkl}\sigma_{kl} + d_{kij}E_k \tag{3}$$

$$D_i = d_{ikl}\sigma_{kl} + \in^{\mathrm{T}}_{ik} E_k \tag{4}$$

$$\varepsilon_{ij} = \frac{1}{2}(u_{j,i} + u_{i,j}) \tag{5}$$

$$E_i = -\phi_i \tag{6}$$

where σ_{ij}, D_i, ε_{ij} and E_i are the stress, electric displacement, strain and electric field intensity, u_i and ϕ are the displacement and electric potential, ρ is the mass density, and s_{ijkl}, d_{kij} and $\in^{\mathrm{T}}_{ik}$ are the elastic compliance, piezoelectric coefficient and dielectric permittivity at constant stress, respectively. A comma followed by an index denotes partial differentiation with respect to the space coordinate x_i or the time t. We have introduced the summation convention for repeated tensor indices. Valid symmetry conditions for the material constants are

$$s_{ijkl} = s_{jikl} = s_{ijlk} = s_{klij},\ d_{kij} = d_{kji},\ \in^{\mathrm{T}}_{ij} = \in^{\mathrm{T}}_{ji} \tag{7}$$

For piezoelectric ceramics which exhibit symmetry of a hexagonal crystal of class 6 mm with respect to principal x_1, x_2, and x_3 axes, the constitutive relations can be written in the following form:

$$\begin{Bmatrix}\varepsilon_1\\ \varepsilon_2\\ \varepsilon_3\\ \varepsilon_4\\ \varepsilon_5\\ \varepsilon_6\end{Bmatrix} = \begin{bmatrix} s_{11} & s_{12} & s_{13} & 0 & 0 & 0\\ s_{12} & s_{11} & s_{13} & 0 & 0 & 0\\ s_{13} & s_{13} & s_{33} & 0 & 0 & 0\\ 0 & 0 & 0 & s_{44} & 0 & 0\\ 0 & 0 & 0 & 0 & s_{44} & 0\\ 0 & 0 & 0 & 0 & 0 & s_{66}\end{bmatrix}\begin{Bmatrix}\sigma_1\\ \sigma_2\\ \sigma_3\\ \sigma_4\\ \sigma_5\\ \sigma_6\end{Bmatrix} + \begin{bmatrix} 0 & 0 & d_{31}\\ 0 & 0 & d_{31}\\ 0 & 0 & d_{33}\\ 0 & d_{15} & 0\\ d_{15} & 0 & 0\\ 0 & 0 & 0\end{bmatrix}\begin{Bmatrix}E_1\\ E_2\\ E_3\end{Bmatrix} \tag{8}$$

$$\begin{Bmatrix}D_1\\ D_2\\ D_3\end{Bmatrix} = \begin{bmatrix} 0 & 0 & 0 & 0 & d_{15} & 0\\ 0 & 0 & 0 & d_{15} & 0 & 0\\ d_{31} & d_{31} & d_{33} & 0 & 0 & 0\end{bmatrix}\begin{Bmatrix}\sigma_1\\ \sigma_2\\ \sigma_3\\ \sigma_4\\ \sigma_5\\ \sigma_6\end{Bmatrix} + \begin{bmatrix} \in^{\mathrm{T}}_{11} & 0 & 0\\ 0 & \in^{\mathrm{T}}_{11} & 0\\ 0 & 0 & \in^{\mathrm{T}}_{33}\end{bmatrix}\begin{Bmatrix}E_1\\ E_2\\ E_3\end{Bmatrix} \tag{9}$$

where

$$\sigma_1 = \sigma_{11}, \sigma_2 = \sigma_{22}, \sigma_3 = \sigma_{33},\ \sigma_4 = \sigma_{23} = \sigma_{32}, \sigma_5 = \sigma_{31} = \sigma_{13},\ \sigma_6 = \sigma_{12} = \sigma_{21} \tag{10}$$

$$\varepsilon_1 = \varepsilon_{11}, \varepsilon_2 = \varepsilon_{22}, \varepsilon_{33}, \varepsilon_3 = \varepsilon_{33},\ \varepsilon_4 = 2\varepsilon_{23} = 2\varepsilon_{32},\ \varepsilon_5 = 2\varepsilon_{31} = 2\varepsilon_{13},\ \varepsilon_6 = 2\varepsilon_{12} = 2\varepsilon_{21} \tag{11}$$

$$s_{11} = s_{1111} = s_{2222}, s_{12} = s_{1122},\ s_{13} = s_{1133} = s_{2233}, s_{33} = s_{3333},\ s_{44} = s_{2323} = s_{3131},\ s_{66} = s_{1212} = 2(s_{11} - s_{12}) \tag{12}$$

$$d_{15} = 2d_{131} = 2d_{223},\ d_{31} = d_{311} = 2d_{322},\ d_{33} = d_{333} \tag{13}$$

2.2. Model

A three-dimensional piezoelectric cantilever model is used for analysis, with two constituent materials: PZT-A and PZT-B (see Fig. 1). Let the coordinate

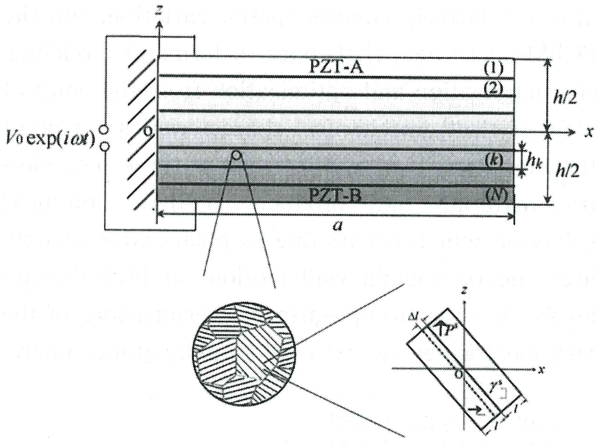

Fig. 1. Sketch of functionally graded piezoelectric cantilever and domain structures

axes $x_1 = x_2$ and $y = x_2$ be chosen such that they coincide with the middle plane of the hybrid laminate and the $z = x_3$ axis is perpendicular to this plane. The functionally graded piezoelectric plate is assumed to have length a and width b in the $x-y$ plane, and thickness h in the z direction. The piezoelectric material is graded through the thickness only, from pure PZT-A at the surface $z=h/2$ to pure PZT-B at $z=-h/2$. The plate is discretized into N layers which are assumed to have constant material properties. The thickness of the kth layer is h_k.

The piezoelectric response due to AC voltage $V_0 \exp(i\omega t)$ consists of the sum of intrinsic and extrinsic effects; V_0 is the AC voltage amplitude and ω is the input frequency. The intrinsic effect refers to the homogeneous deformation caused by the electric field, and the extrinsic effect results from the elastic deformation caused by the motions of domain walls. For simplicity here, the AC electric field $E_z = E_0 \exp(i\omega t)$ is parallel to the direction of spontaneous polarization P^s in one of the domains; E_0 is the AC electric field amplitude. A domain wall displacement gives rise to the changes of the strain and electric dipole moment. The induced strain $\Delta\varepsilon_{11}$ and polarization ΔP_3 by the domain wall motion of the actuator are given by[4]

$$\Delta\varepsilon_{11} = \Delta s_{11}\sigma_{11} + \Delta d_{311}E_3 \tag{14}$$

$$\Delta P_3 = \Delta d_{311}\sigma_{11} + \Delta \in_{33}^{T} E_3 \tag{15}$$

where

$$\Delta s_{11} = \frac{\gamma^{s2}}{2lf_D},\ \Delta d_{311} = \frac{\gamma^s P^s}{2lf_D},\ \Delta \in_{33}^{T} = \frac{P^{s2}}{2lf_D} \tag{16}$$

In Eq. (16), γ^s is the spontaneous strain, l is the domain width and f_D is the force constant for the domain wall motion process. The strain ε_{11} and electric displacement D_3 become

$$\varepsilon_{11} = s_{11}^{*}\sigma_{11} + s_{12}\sigma_{22} + s_{13}\sigma_{33} + d_{31}^{*}E_3 \tag{17}$$

$$D_3 = d_{31}^{*}\sigma_{11} + d_{31}\sigma_{22} + d_{33}\sigma_{33} \in_{33}^{T^*} E_3 \tag{18}$$

where

$$s_{11}^{*} = s_{11} + \Delta s_{11},\ d_{31}^{*} = d_{31} + \Delta d_{311},\ \in_{33}^{T^*} = \in_{33}^{T} + \Delta \in_{33}^{T} \tag{19}$$

The extrinsic dielectric constant $\Delta \in_{33}^{T}$ is described by [3]

$$\Delta \in_{33}^{T} = \in_{33}^{T} \frac{2E_0}{3E_c} \tag{20}$$

where E_c is a coercive electric field.

In the numerical examples, the functionally graded model[1] concerning the material inhomogeneity is employed. The material constants of the kth layer for N layered FGPMs

$$\begin{aligned} (s_{ijkl})_k &= s_{ijkl}^{A} V_k + s_{ijkl}^{B}(1-V_k) \\ (d_{ikl})_k &= d_{ikl}^{A} V_k + d_{ikl}^{B}(1-V_k) \\ (\in_{ik}^{T})_k &= \in_{ik}^{TA} V_k + \in_{ik}^{TB}(1-V_k) \end{aligned} \tag{21}$$

where the superscripts A and B represent the materials PZT-A and PZT-B, respectively, and

$$V_k = \left(\frac{k-1}{N-1}\right)^{1/m} \tag{22}$$

In Eq. (22), m is the functionally graded material volume fraction exponent, and governs the distribution pattern of the electroelastic properties across the thickness of the FGPMs.

We performed finite element calculations to obtain the deflection, induced voltage and internal stresses for the functionally graded piezoelectric sensors and actuators. The commercial software ANSYS with PLANE 13 coupled-field solid elements was employed in the analysis. From Eqs. (16), (19) and (20), the elastic compliance $(s_{11}^{*})_k = (s_{11})_k + (\Delta s_{11})_k$, piezoelectric coefficient $(d_{31}^{*})_k = (d_{31})_k + (\Delta d_{311})_k$ and dielectric permittivity $(\in_{33}^{T^*})_k = (\in_{33}^{T})_k + (\Delta \in_{33}^{T})_k$ vary with domain wall motion. To get $(\Delta s_{11})_k$, $(\Delta d_{311})_k$ and $(\Delta \in_{33}^{T})_k$, $P^s = 0.3$ C/m^2 and $\gamma^s = 0.004$ are used. Making use of electric field dependent piezoelectric material properties, the model calculated the nonlinear behavior.

3. EXPERIMENTAL PROCEDURE

Functionally graded piezoelectric bimorph was prepared using soft PZTs C-91 and C-6 (Fuji Ceramics Ltd. Co. Japan)[3]. The coercive electric fields of C-91 and C-6 are 0.35 and 0.45 MV/m, respectively. Consider two types of grading through the thickness, type I where the piezoelectric properties increase toward the mid-plane, and type II where the piezoelectric properties decrease toward the mid-plane. The PZT C-91 is characterized by high piezoelectric constants and low coercive electric field. 3-layered FGPMs of thickness $h_1 + h_2 + h_3 = 0.21$ mm and $h_4 + h_5 + h_6 = 0.21$ mm are respectively added to the upper and lower surfaces of an electrode film to make the 6-layered parallel

bimorph. The bimorph has also electrodes on both sides. The thickness of each layer is about h_k = 0.07 mm (k =1, ..., 6), and m is taken to be 1. The specimen has a length of 55 mm, a width of 20 mm and a thickness of 0.42 mm. We also consider the 6-layered inward series bimorph.

First, the amplitude of the dynamic deflections of the functionally graded piezoelectric actuators was measured with a microscope (see Fig. 2(a)). The free length is 40 mm. The top and center electrodes were grounded, while a voltage was applied to the surface electrode of the lower element. Next, a deflection w_0 was applied at x=40 mm, y=0 mm and z=0.23 mm as shown in Fig. 2(b). To measure the induced voltage across the sample, one channel of an oscilloscope was connected directly across the lower element. The free length was set to 43 mm.

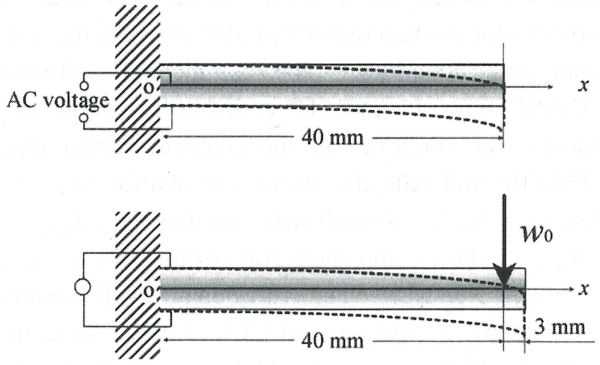

Fig. 2. Experimental setup: (a) bimorph actuator (b) bimorph sensor

4. RESULTS AND DISCUSSION

Fig. 3 shows the tip deflection w_{tip} as a function of AC voltage V_0 at frequency $f = \omega/2\pi$ = 60 Hz for 6-layered parallel bimorphs (m =1) with a symmetric construction of Type I [C-6/.../C-91]$_s$ and type II [C-91/.../C-6]$_s$, where [ ]$_s$ designates symmetry about the middle surface. The results obtained from the finite element method (FEM) and tests are shown, and a, b and h are taken to be 40, 20 and 0.42 mm, respectively, in the simulations presented. The results for type II [C-91/.../C-6]$_s$ series bimorph are also presented. The tip deflection of type I [C-6/.../C-91]$_s$ parallel bimorph is larger than that of type II [C-91/.../C-6]$_s$ parallel and series bimorphs. Comparing the calculation results of the type II parallel and series bimorphs, no difference is observed. It is shown that the trend is sufficiently similar between the analyses and experiments. Fig. 4 shows the tip deflection versus AC voltage at 60 Hz for 10-layered type I parallel bimorphs (m=1, 2). The tip deflection increases with increasing functionally graded material volume fraction exponent. On the other hand, the number of layers has small effect on the tip deflection (not shown).

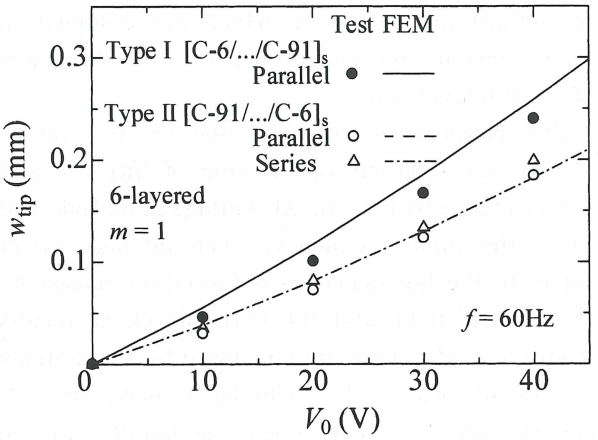

Fig. 3. Tip deflection vs ac voltage at 60 Hz for 6-layered type I and II actuators (m=1)

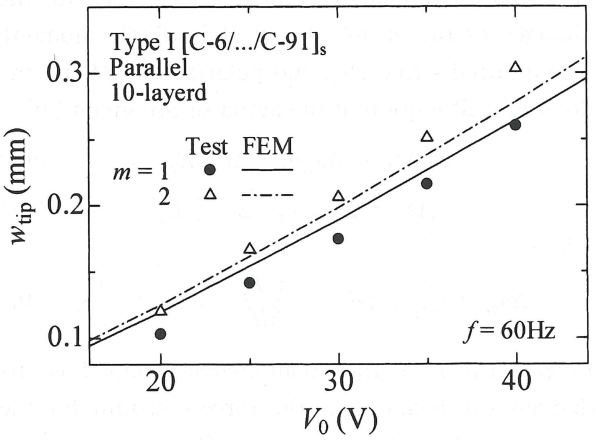

Fig. 4. Tip deflection vs ac voltage at 60 Hz for 10-layered type I actuators (m=1, 2)

Fig. 5 shows the induced voltage versus applied deflection w_0 for 6-layered type I and II parallel bimorphs (m=1). Larger induced voltage is found in the type I bimorph sensor. The calculation results are in good agreement with experimental measurements.

The variations of normal stress σ_{xx} along the thickness direction are calculated for the 6-layered type I and II bimorphs (m=1) at a chosen point (x= 20 mm and y =0 mm) and the results are shown in

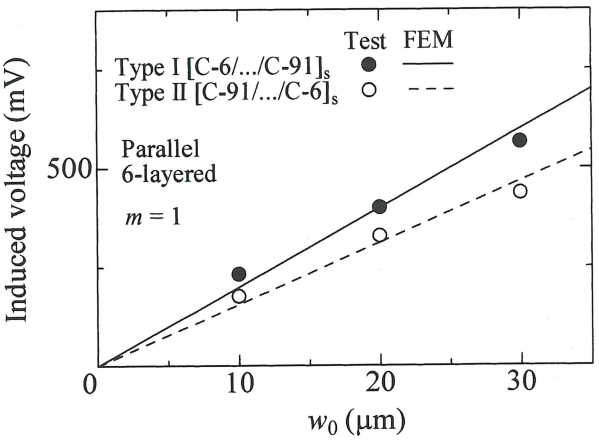

Fig. 5. Induced voltage vs applied deflection for 6-layered type I and II sensors ($m=1$)

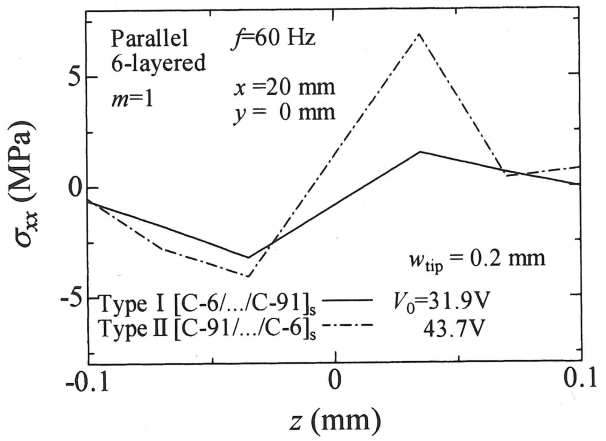

Fig. 6. Distributions of normal stress σ_{xx} along the thickness direction under a deflection of 200 μm at 60 Hz for 6-layered type I and II actuators ($m=1$)

Fig. 6. All calculations were chosen at w_{tip} = 200 μ m and $f=60$ Hz. The driving voltages of the bimorphs under $w_{tip}=200$ μm are about 31.9 V for the type I and 43.7 V for the type II. The lower stress is noted for the type I parallel bimorph.

5. CONCLUSIONS

A numerical and experimental investigation of the FGPMs under electromechanical loading was conducted. On the basis of the study conducted, the following conclusions may be inferred:

1. The functionally graded material volume fraction have influence of the detection and response of the FGPMs.

2. When the piezoelectric properties increase toward the mid-plane of the functionally graded bimorphs, functional grading of piezoelectric materials could effectively increase the tip deflection and induced voltage, and reduce the magnitude of internal stresses.

As a remark, we note that this study may be useful in designing advanced piezoelectric devices.

Acknowledgments

This work was partially supported by the Grant-in-Aid for Scientific Research (B) and Young Scientists (B) from the Ministry of Education, Culture, Sports, Science and Technology, Japan.

REFERENCES

1) M. Taya, A. A. Almajid, M. Dunn, H. Takahashi, Design of bimorph piezo-composite actuators with functionally graded microstructure, *Sens. Actuators A*, **107(3)** (2003) 248-260.

2) F. Narita, Y. Shindo, K. Hayashi, Bending and polarization switching of piezoelectric laminated actuators under electromechanical loading, *Comput. Struct.*, **83(15/16)** (2005) 1164-1170.

3) F. Narita, Y. Shindo, M. Mikami, Analytical and experimental study of nonlinear bending response and domain wall motion in piezoelectric laminated actuators under ac electric fields, *Acta. Mater.*, **53(17)** (2005) 4523-4529.

4) G. Arlt, H. Dederichs, Complex elastic, dielectric and piezoelectric constants by domain wall damping in ferroelectric ceramics, *Ferroelectrics*, **29** (1980) 47-50.